The liquid-solid transition of hard discs: first-order transition or Kosterlitz-Thouless-Halperin-Nelson-Young scenario?

2002 J. Phys.: Condens. Matter 14 2323

(http://iopscience.iop.org/0953-8984/14/9/321)

INSTITUTE OF PHYSICS PUBLISHING JOURNAL OF PHYSICS: CONDENSED MATTER

J. Phys.: Condens. Matter **14** (2002) 2323–2333 PII: S0953-8984(02)32439-1

The liquid–solid transition of hard discs: first-order transition or Kosterlitz–Thouless–Halperin–Nelson–Young scenario?

Kurt Binder[1], **Surajit Sengupta**[1,2] **and Peter Nielaba**[3]

[1] Institut für Physik, Johannes Gutenberg Universität Mainz, Staudinger Weg 7, D-55099 Mainz, Germany
[2] Condensed Matter Group, SN Bose National Centre for Basic Sciences, JD Block, Sect. 3, Salt Lake City, Calcutta-700091, India
[3] Fakultät für Physik, Universität Konstanz, Fach M 691, D-78457 Konstanz, Germany

Received 8 January 2002
Published 22 February 2002
Online at stacks.iop.org/JPhysCM/14/2323

Abstract

We consider the question of whether a two-dimensional hard-disc fluid has a first-order transition from the liquid state to the solid state as in the three-dimensional melting–crystallization transition or whether one has two subsequent continuous transitions, from the liquid to the hexatic phase and then to the solid phase, as proposed by Kosterlitz, Thouless, Halperin, Nelson and Young (KTHNY). Monte Carlo (MC) simulations of the fluid that study the growth of the bond orientational correlation length, and of the crystal are discussed.

The emphasis is on a recent consistency test of the KTHNY renormalization group (RG) scenario, where MC simulations are used to estimate the bare elastic constants and dislocation fugacities in the solid, as a function of density, which then are used as starting values for the RG flow. This approach was validated earlier for the XY model as well.

1. Introduction

Although the system of hard discs in two dimensions is one of the simplest models of a fluid, it nevertheless exhibits a rich and complex behaviour: the problem that needs to be considered is that of phase transitions driven by the formation of topological defects and the possible occurrence of a hexatic phase [1–7]. The present paper describes attempts by Monte Carlo (MC) simulation to clarify this problem.

In section 2, the problem will be introduced in more detail, and the most pertinent theoretical predictions will be summarized. Then simulation studies of the fluid phase and the evidence for a possible divergence of the bond orientational susceptibility will be

discussed [8–10] (section 3). As an intermezzo (section 4), a study of the two-dimensional planar rotor model [11] will be mentioned: for this model it is widely believed—though not firmly proven—that a Kosterlitz–Thouless (KT) transition [1] driven by vortex–antivortex unbinding does occur. By adopting a new way [11] to combine renormalization group (RG) ideas with MC 'input', a powerful technique for characterizing the transition is obtained. An approach in the same spirit is then (section 5) used on the solid phase of the hard-disc system, in order to show that the MC results are compatible with the possible existence of a hexatic phase. Section 6, finally, summarizes a few conclusions.

2. Two-dimensional solid–liquid transitions and bond orientational order

For hard discs, the potential energy U is infinite if two discs (of diameter $\sigma = 1$) overlap, while otherwise $U = 0$. So temperature essentially plays no role here, since there is no finite energy scale, and the only nontrivial control parameter still left is the density ρ in the system. Therefore it was a nontrivial discovery—made by molecular dynamics simulation [12] long ago—that a transition from a fluid phase at low density to a high-density crystal (with triangular lattice structure) does indeed occur. While the early studies [12, 13] concluded that this transition is a first-order transition (like in the three-dimensional case), the validity of this conclusion is doubtful, since the early work relied on studies of a few hundred particles only, and with the computer resources at that time a serious study of finite-size effects could not have been attempted. Also, no study of bond orientational order was carried out [12,13]. More recent theories show [3–7] that a discussion of bond orientational order is crucial, however.

Note that in general a crystal is characterized both by positional long-range order and by bond orientational long-range order [3–7]. In $d = 2$ dimensions, however, rigorous theorems [14] exclude positional long-range order (for $\rho < \rho_{cp} = 2/\sqrt{3}$, where ρ is the density of the close-packed structure; note that the hard-sphere diameter is our unit of length), while orientational long-range order can still occur.

In order to define the bond orientational order parameter, imagine a Voronoi construction carried out between the centres of mass of a disc and its neighbours. In this way, nearest neighbours can unambiguously be defined for each configuration, and the straight line connecting the centres of mass of two nearest neighbours is called a bond. Taking the direction of a bond between particle k and one of its neighbours as a reference direction for the whole lattice, we define the angle between the bond connecting particle k and one of its nearest neighbours j and the reference direction as ϕ_{kj}. For a perfect triangular structure, ϕ_{kj} will be $2\pi/6$ or a multiple thereof. Therefore it makes sense to define the order parameter Ψ as

$$\Psi = \left| \sum_k \Psi_k \right| \Big/ N, \qquad \Psi_k = (1/6) \sum_{j\,(\text{n.n. of } k)} \exp(6\mathrm{i}\phi_{jk}), \tag{1}$$

N being the particle number in the system. For a perfect triangular structure, $\Psi_k = 1$ for all k and $\Psi = 1$, while in the disordered phase the Ψ_k become complex numbers and Ψ will average to zero for $N \to \infty$.

But in the disordered phase it still makes sense to study the bond orientational correlation function

$$g_6(r) = |\langle \Psi_k \Psi_\ell \rangle|, \qquad r = |\vec{r}_k - \vec{r}_\ell|. \tag{2}$$

According to the RG theory proposed by Halperin, Nelson and Young [3–7], melting in $d = 2$ dimensions can occur via two continuous transitions (at densities ρ_ℓ and ρ_s) with corresponding pressures p_ℓ and $p_s > p_\ell$, rather than via a single first-order transition at pressure p_t (where a fluid of density ρ'_ℓ and a solid of density ρ'_s will coexist); see figure 1. Both in the fluid phase

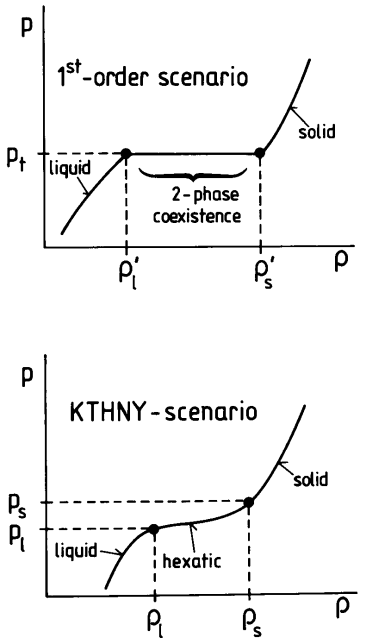

Figure 1. Qualitative isotherms where the pressure p is plotted versus density ρ, for the case of a first-order transition (upper part) and according to the KTHNY theory (lower part). Note that for the hard-disc system there is no temperature dependence, so one can choose $k_B T \equiv 1$.

and in the hexatic phase, $\langle \Psi \rangle = 0$, but the behaviours of $g_6(r)$ are different: in the fluid one finds an exponential decay, while there is a power-law decay in the hexatic phase:

$$g_6(r \to \infty) \propto \exp(-r/\xi), \qquad \rho < \rho_\ell, \tag{3}$$

$$g_6(r \to \infty) \propto r^{-\eta}, \qquad \rho_\ell \leqslant \rho < \rho_s, \tag{4}$$

and the correlation length ξ of the bond orientational order diverges according to a KT behaviour [1–7] as ρ_ℓ is approached, as does the bond orientational susceptibility $\chi \equiv \int \mathrm{d}^2\vec{r}\, g_6(r)$:

$$\ln \xi \propto \ln \chi \propto (\rho_\ell - \rho)^{-1/2}. \tag{5}$$

Conversely, if one has a first-order transition, both ξ and χ stay finite at ρ_s, and a nonzero order parameter $\langle \Psi \rangle$ has already started to increase (linearly in the density) at ρ_ℓ' (according to the lever rule), while according to the Kosterlitz, Thouless, Halperin, Nelson and Young (KTHNY) scenario, $\langle \Psi \rangle$ is nonzero for $\rho > \rho_s$ only.

The mechanism of these continuous phase transitions is the unbinding of topological defects. Just as in the two-dimensional XY ferromagnet or planar rotor model, where vortex–antivortex unbinding occurs [1, 5], the transition from the solid to the hexatic phase is driven by the unbinding of dislocation pairs with oppositely oriented Burgers vectors. While a free dislocation would have an infinitely long extra half-row of atoms, such a dislocation pair at finite distance involves a finite number of atoms in the extra row only, and such an excitation hence costs only a finite energy and can occur in the crystal in thermal equilibrium. The hexatic phase then melts into the liquid via disclination pair unbinding.

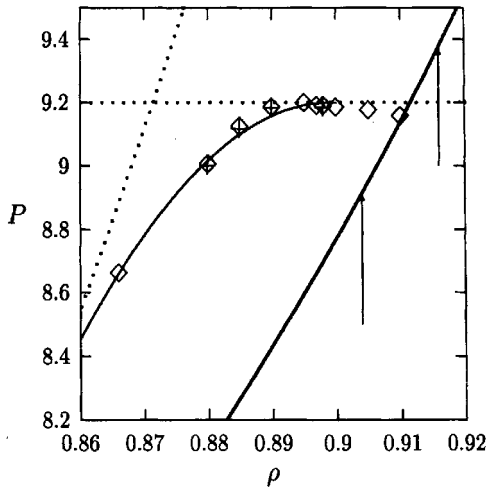

Figure 2. The equation of state of the hard-disc fluid in the transition region. Diamonds and crosses represent data from Jaster [10] for systems of 128×128 and 256×256 particles, respectively, while the thin solid curve is a polynomial fit to these data for $\rho \leqslant 0.9$ (data for $\rho > 0.9$ may be invalid due to finite-size effects and insufficient equilibration). The horizontal dotted line $p = 9.2$ indicates the resulting estimate for P_t (or p_ℓ). The other dotted curve is a semiempirical form for the equation of state [16] that provides a good fit of the MC data [17] for $0 < \rho < 0.8$. The thick solid curve is the pressure of the solid phase, obtained via thermodynamic integration [15], the lower arrow showing the position of the solid-to-hexatic transition if the bare (unrenormalized) Young's modulus K is used in the KTHNY theory, while the upper arrow shows the location of this transition if the renormalized value K_R is used (see section 5) (from Sengupta *et al* [15]).

3. Simulation studies of the liquid phase and evidence for bond orientational order

Figure 2 shows an attempt to distinguish between the two scenarios of figure 1 using the most recent MC results [10–15]. It is immediately obvious that the data support neither scenario strongly: if there were a first-order transition, the p versus ρ curve should exhibit a kink at ρ_ℓ' and stay flat from there on. However, it is apparent that instead the slope $\mathrm{d}p/\mathrm{d}\rho$ gets gradually smaller, and there is no kink (note that at $\rho = 0.89$ and $\rho = 0.895$ there is no sign of any two-phase coexistence whatsoever yet; all the criteria indicate that one is still in the fluid phase). Note also that the smooth decrease of $\mathrm{d}p/\mathrm{d}\rho$ near $\rho = 0.89$ is not due to finite-size rounding—data for two large system sizes differing by a factor of two in their linear dimension coincide. As will be discussed shortly, the best estimate for the divergence of χ compatible with equation (5) is $\rho_\ell = 0.899$ [9]. However, the slight decrease of p seen in the data for $0.9 \leqslant \rho \leqslant 0.91$ clearly is not compatible with the KTHNY scenario (figure 1): if this decrease were to persist for the thermal equilibrium properties of still larger systems, it would be a rather clear evidence that a two-phase coexistence region of a first-order transition has been entered. However, at this point it is not clear whether this decrease is a real effect or just an artefact of insufficient equilibration or too-small system sizes in the region $\rho > \rho_\ell$ (due to the power law, equation (4), finite-size effects are expected to be far more pronounced in the hexatic phase than in the other phases).

Figure 3 presents the MC results for the bond orientational order parameter, as obtained from a subbox finite-size scaling analysis [8]. This subbox method was used (i) since a single large-scale simulation (using $N = 16\,384$ hard discs and a statistical effort of 10^6 Monte Carlo steps (MCS) per particle) yields simultaneously finite-size data for a broad range of sizes and

(ii) since—because the boundaries of the subboxes are only virtual and have no constraining physical effect—density fluctuations in the subboxes are not suppressed, corresponding to an equilibrium within the subboxes at constant chemical potential μ as long as $M_b \gg 1$. It is seen that finite-size effects on $\langle\Psi\rangle_L$ are negligible for $\rho \geqslant 0.91$, so the densities can safely be identified as the solid phase. On the other hand, for $\rho \leqslant 0.89$ it is clear that $\langle\Psi\rangle_L \to 0$ for $L \to \infty$; so if there were a first-order transition, ρ'_ℓ should be somewhat larger than 0.89, and ρ'_s should be somewhat smaller than 0.91. Already these bounds yield a width of a possible two-phase coexistence region smaller than previous estimates [12,18]. In addition, one expects to see a rather sharp kink at $\rho = \rho'_s$ (figure 3(*b*)), but such a kink cannot be identified from the data either (of course, the kink at $\rho = \rho'_\ell$ is expected to be blurred by finite-size effects, since $\langle\Psi\rangle_L$ must be nonzero for any $L < \infty$).

Also, the distribution function $P_L(\Psi, \rho)$ was monitored, in order to check for signals of a double-peak structure, one peak near $\Psi = 0$ coexisting with a peak near $\Psi = 0.6 - 0.7$: however, no such evidence for phase coexistence [19] could be detected. On the other hand, the fourth-order cumulant [19, 20]

$$U_L = 1 - \langle\Psi^4\rangle/[3\langle\Psi^2\rangle^2] \tag{6}$$

is compatible with a continuous transition at $\rho_\ell = 0.8985 \pm 0.0005$ [8] (figure 4). While the subsystem analysis [8] yielded reliable data for χ only in the range $\chi \leqslant 20$, and fitting these data to equation (5) indicated $\rho_\ell = 0.913$, which would imply that χ is still finite at the actual transition density $\rho_\ell \approx 0.8985$, more extensive data for χ due to Jaster [9] covering the range up to $\chi \approx 10^3$ show that χ is indeed compatible with equation (5) for $\rho_\ell \approx 0.899$. A finite-size scaling analysis of χ for various densities near ρ_ℓ yielded further support for a KT-type divergence of χ at this density. Considered together with figure 4, we take this as compelling evidence for a continuous KT-type transition from the fluid phase to another phase at $\rho_\ell \approx 0.899$. However, in view of figures 1, 2 it is clear that any evidence that this other phase is a hexatic phase is still lacking.

4. Monte Carlo input for renormalization group treatments of Kosterlitz–Thouless transitions: the case of the planar rotor model

In this section, we make a detour in order to present a new method for exploring KT transitions. The basic idea is to check the self-consistency of the RG flow equations that describe this problem [21, 22] (figure 5) using the appropriate MC 'input'. We test here the viability of such an approach for the planar rotor model on the square lattice, whose Hamiltonian is (the exchange energy is set to unity)

$$H = -\sum_{\langle i,j\rangle} \cos(\phi_i - \phi_j), \qquad 0 \leqslant \phi_i < 2\pi. \tag{7}$$

The theory [1] can be cast in the framework of a two-parameter renormalization flow for the spin-wave stiffness $K(\ell)$ and the fugacity of vortices $y(\ell)$, where ℓ is related to the length scale considered, r, as $\ell = \ln(r/a)$, where a is the lattice spacing. Absorbing a factor $1/k_BT$ in K, it is predicted [21] that $K_c = K(T_c) = 2/\pi$ is a universal constant. Therefore it is convenient to write the flow equations in terms of the scaled variables $x = 2 - \pi K$ and $y' = 4\pi y$. To leading and next-to-leading order these equations are [22]

$$\mathrm{d}x/\mathrm{d}\ell = y'^2 - y'^2 x, \qquad \mathrm{d}y/\mathrm{d}\ell = xy' + (5/4)y'^3. \tag{8}$$

Figure 5 shows numerical solutions to these flow equations, starting from states of the model on the smallest possible scale—that of the lattice spacing, for which there are no vortices, and the corresponding 'bare' spin-wave stiffness $K(0)$ and vortex fugacities $y(0)$. These starting

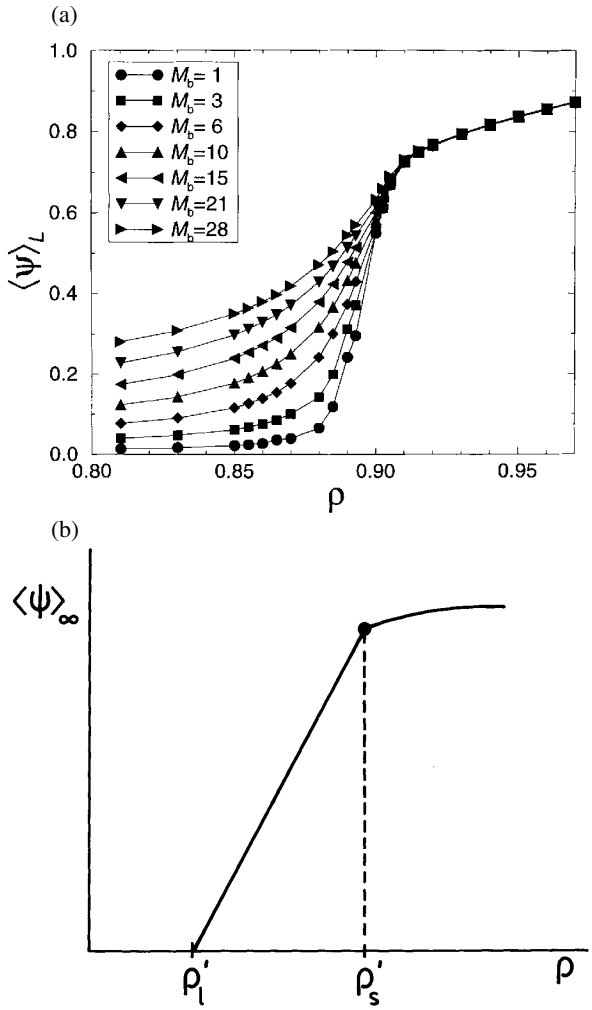

Figure 3. (*a*) First moment of the bond orientational order parameter $\langle\Psi\rangle_L$ of the hard-disc fluid as a function of density ρ for selected subbox sizes $L = S/M_b$ (values of M_b are given in the key), for an $S \times S$ system with periodic boundary conditions containing $N = 16\,384$ particles. Note that the shape of the simulation box is a parallelepiped compatible with the triangular lattice structure, and the parameter M_b is equal to the number of subboxes along the edge of the total system. Lines are guides to the eye. From Weber *et al* [8]. (*b*) A schematic diagram of the variation of $\langle\Psi\rangle_\infty$ expected in the case of a first-order transition.

values were obtained from specially constrained MC simulations of the model that will be explained below. One sees from figure 5 that the flow lines to the right of the separatrix all flow to $y' = 0$, i.e. a state with no free vortices on large length scales: this is the low-temperature phase. The flow lines to the left of the separatrix, however, bend over and flow to large y': this means the disordered phase! But from the MC simulation we know which temperature belongs to each starting state—in particular, we know also the temperature which falls on the separatrix, which is $T_c = 0.899$. This estimate is in excellent agreement with careful large-scale direct MC simulations of the model, which yielded [23–26] $T_c = 0.895 \pm 0.005$. The data also yielded an estimate for the constant b in the law $\xi \propto \exp[bt^{-1/2}]$ where now

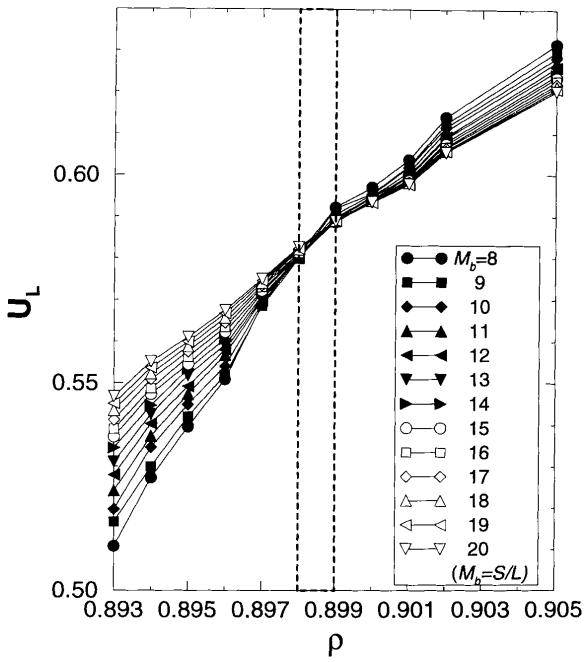

Figure 4. Order parameter cumulants U_L as a function of the total density ρ for various subsystem sizes $L = s/M_b$. The lines connecting the data points are guides to the eye. The vertical dashed line mark the range within which the cumulant intersection occurs (from Weber *et al* [8]).

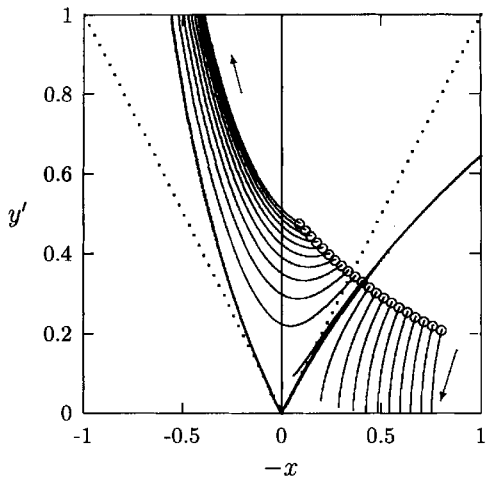

Figure 5. Flows of $x = 2 - \pi K$ and $y' = 4\pi y$ where K is the spin-wave stiffness and $y = \exp(-\mu/k_B T)$ the fugacity of vortices under the action of the RG, starting from a set of initial conditions (circles) obtained from the simulation of the planar rotor model, equation (7). The dotted lines ($y' = \pm x$) show the separatrix for the linearized flow equations valid for flows near the fixed point $x = 0$, $y = 0$; the thick lines show the actual separatrix for the nonlinear equations, equation (8). Note that these curves separate flows that terminate on the critical line $x < 0$, $y = 0$ (ordered phase) from flows towards $y \to \infty$ (disordered phase). Arrows show the direction of the flow (from Sengupta *et al* [11]).

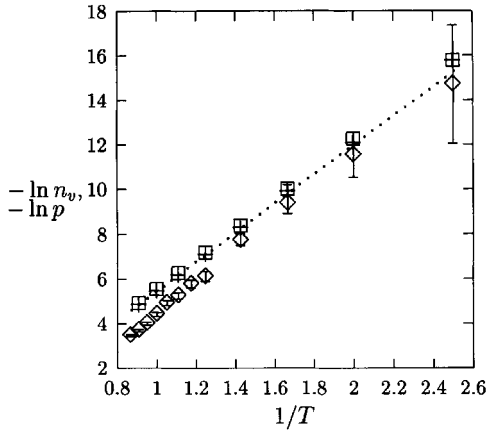

Figure 6. A plot of $-\ln(n_v)$ and $-\ln(p)$ versus the inverse temperature. The vortex concentration n_v (diamonds) is calculated in the unconstrained simulation of equation (7) for $L \times L$ lattices ($L = 100$), and is subject to large errors at low T. The rejection ratio p in the constrained simulation was calculated for $L = 60$ (+) and $L = 100$ (□), the errors being smaller than the size of the symbols. The dotted line represents a fit to the latter data (near the transition temperature) yielding $2\mu = 6.55 \pm 0.03$ (from Sengupta *et al* [11]).

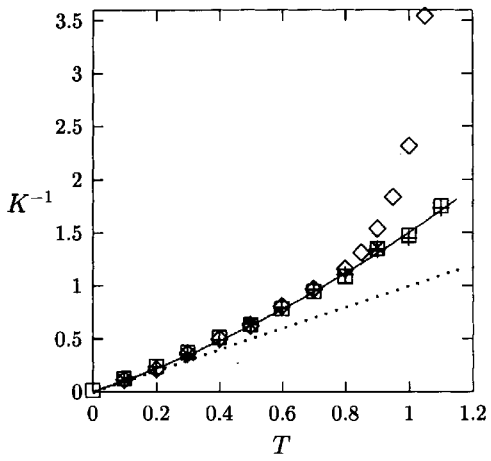

Figure 7. The inverse spin-wave stiffness $K^{-1}(T)$ plotted versus T, for two types of simulation: (i) the unconstrained $L \times L$ lattice with $L = 100$ (diamonds), (ii) the constrained (vortex-free) system for $L = 30$ (×), 60 (+) and 100 (squares), respectively. The dotted straight line is the result from harmonic spin-wave theory, $K^{-1} = T$, while the full curve is a fit to the form $K^{-1} = T + aT^2$ with $a = 0.50 \pm 0.01$ (from Sengupta *et al* [11]).

t is $t = T/T_c - 1$, namely [11] $b = 1.534 \pm 0.002$, in fair agreement with the direct estimate [25] $b = 1.585 \pm 0.009$ (note that the quoted error bars just indicate errors resulting from least-squares fits that do not include the unknown systematic error due to a slightly inaccurate determination of T_c in both cases, and hence one should not place too much reliance on them). We emphasize, however, that for the quoted accuracy of T_c it is essential that the next-to-leading order in equation (8) is included—had we taken the leading order only (dotted-line separatrix in figure 5), a rather inaccurate estimate of T_c would result, namely $T_c = 0.925$ [11].

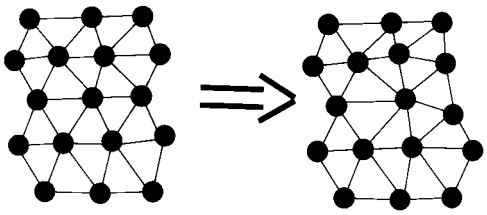

Figure 8. A typical move which attempts to change the coordination number (note the atoms with fivefold and sevenfold coordination), implying the creation of a dislocation pair with opposite Burgers vectors. Such moves are rejected in the simulation, and their rejection rate is measured (from Sengupta *et al* [15]).

Figures 6, 7 now show the MC results on which this treatment is based. The treatment implies a MC simulation of equation (7) where vortex formation is suppressed. This is done as follows: the simulation is always started from a perfectly aligned ferromagnetic state (all $\phi_i = 0$), which has no vortices. Then a site is picked at random, and a move $\phi_i \rightarrow \phi_i'$ is attempted, with $0 \leqslant \phi_i' < 2\pi$. First the standard Metropolis criterion for the acceptance of the move is applied. If a move is being considered for acceptance, we check whether it would create a vortex–antivortex pair. For this purpose, consider all four elementary plaquettes to which the site i belongs. In each plaquette, label the sites anticlockwise as $k = 1, 2, 3, 4$ and define $\Delta\phi_k = \phi_{k+1} - \phi_k$ (with $\phi_5 \equiv \phi_1$). If $\sum_{k=1}^{4} \Delta\phi_k = 0$ for all four plaquettes, no vortex–antivortex pair was created, and the move can indeed be accepted. However, if we find $\sum_{k=1}^{4} \Delta\phi_k = \pm 2\pi$ for any of the plaquettes, a vortex (or antivortex) would be created, and the move must be rejected. The rejection rate p due to this no-vortex constraint is sampled and compared to the vortex concentration n_v in an unconstrained simulation (figure 6). The (inverse) stiffness constant is simply given as $K^{-1} = 4\pi \ln\langle M^2\rangle / N$, where M is the magnetization of the lattice which has $N = L \times L$ sites (figure 7). While K^{-1} would show a singularity at T_c in the unconstrained system (jump from $\pi/2$ to infinity), $[K(0)]^{-1}$ is perfectly smooth near T_c and not plagued by finite-size effects, since the constrained system is not critical there!

5. Melting of the crystal into the hexatic phase

The same idea as was pursued in the previous section for the planar rotor model and its disordering via vortex–antivortex unbinding is now invoked for the study of the melting of the triangular crystal lattice [15]. Again the trick is to apply a constraint that forbids the creation of dislocation pairs (figure 8), measure the rejection rate due to this constraint and estimate the dislocation core energy E_c from this rate:

$$p \equiv p_{pair} = \exp(-2E_c/k_BT)/Z(K) \tag{9}$$

where K is the dimensionless Young's modulus, and $Z(K)$ the 'internal partition function' of a dislocation pair which is (using $k_BT \equiv 1$ again) [27]

$$Z(K) = [2\pi\sqrt{3}/(K/8\pi - 1)]I_0(K/8\pi)\exp(K/8\pi) \tag{10}$$

where I_0 is a Bessel function. From p we hence obtain $y = \exp[-E_c(K)]$, which is one input in the RG flow equation [2–7]. The elastic constants of the defect-free solid were measured by a new subblock technique that is described elsewhere [28]. In this way, K could be obtained with high precision over the whole density range of interest ($0.88 \leqslant \rho \leqslant 1.1$) [15]. Figure 9 now is the analogue of the flow diagram for the plane rotor model (figure 5). Note that the universal fixed-point value is $K = 16\pi$ here. Therefore figure 10 plots both the starting value

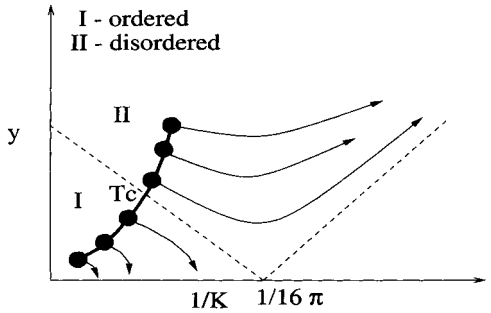

Figure 9. Schematic flows of the dimensionless Young's modulus K and the dislocation fugacity y according to the KTHNY recursion relations. The dashed lines show the separatrix whose intersection with the line of initial states (the solid line connecting the full circles $y(\ell = 0)$ and $K^{-1}(\ell = 0)$ at different temperatures T or densities ρ, respectively) determines the transition point (T_c or ρ_c, respectively) (from Sengupta *et al* [15]).

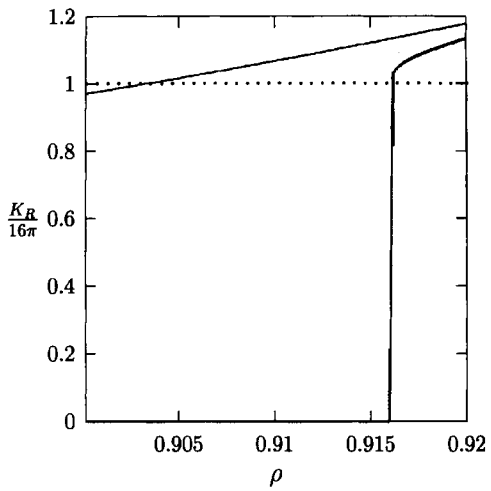

Figure 10. Bare Young's modulus $K(0)/16\pi$ (upper curve) and renormalized modulus $K_R/16\pi$ (lower curve) plotted versus density. The dotted horizontal line $K/16\pi = 1$ highlights the value at which the solid-to-hexatic transition is predicted (from Sengupta *et al* [15]).

$K(0)/16\pi$ and the renormalized value $K_R/16\pi$, as obtained from the recursion relations: in this way one would obtain an estimate $\rho_s = 0.916$ and (figure 2) $p_c = 9.39$. Of course, the known recursion relations [2–7] contain only the leading terms, and experience with the planar rotor model indicates that the neglect of the next-to-leading terms implies significant errors. Therefore it is likely that the true result for $K_R/16\pi$ in figure 10 lies somewhere in between the first-order result and the unrenormalized value (which would imply a transition at $\rho = 0.904$, which also exceeds $\rho_\ell = 0.899$, but is not a reasonable estimate for ρ_s because the corresponding pressure would be too low (figure 2)). In view of these considerations, we suggest $\rho_s = 0.914 \pm 0.002$ as a preliminary estimate for the location of the phase boundary between the solid and hexatic phases.

6. Concluding remarks

In this paper, we have discussed the evidence for the applicability of the KTHNY theory to the melting/crystallization transition of the hard-disc fluid. It has been shown that the currently available simulation data are compatible with a continuous transition from the fluid to the hexatic phase (with divergent bond orientational susceptibility) at $\rho_\ell \approx 0.899$, and with a hexatic-to-crystal transition at $\rho_s \approx 0.914 \pm 0.002$. However, no simulations that reach full thermal equilibrium in the density range $0.90 \leqslant \rho \leqslant 0.915$ and show directly the existence of the hexatic phase are available so far. Without such direct evidence, the possibility of a (very weak) first-order transition from the fluid to the crystal cannot yet be firmly ruled out, although so far clear signals of two-phase coexistence are also lacking.

Acknowledgments

We are particularly grateful to D Marx and H Weber for their fruitful collaboration in early stages of this work [8]. We thank H C Andersen, D Frenkel, M Bates, M Rao, W Janke and D R Nelson for stimulating interaction. This research originated while one of us (SS) was supported by an Alexander von Humboldt fellowship. PN acknowledges support from the Deutsche Forschungsgemeinschaft (DFG) via Sonderforschungsbereich 513.

References

[1] Kosterlitz J M and Thouless D J 1973 *J. Phys. C: Solid State Phys.* **6** 1181
[2] Halperin B I and Nelson D R 1978 *Phys. Rev. Lett.* **41** 121
[3] Nelson D R and Halperin B I 1979 *Phys. Rev.* B **19** 2457
[4] Young A P 1979 *Phys. Rev.* B **19** 1855
[5] Nelson D R 1983 *Phase Transitions and Critical Phenomena* vol 7, ed C Domb and J L Lebowitz (London: Academic)
[6] Strandburg K J 1988 *Rev. Mod. Phys.* **60** 161
[7] Kleinert H 1989 *Gauge Fields in Condensed Matter* (Singapore: World Scientific)
[8] Weber H, Marx D and Binder K 1995 *Phys. Rev.* B **51** 14 636
[9] Jaster A 1999 *Europhys. Lett.* **42** 277
[10] Jaster A 1999 *Phys. Rev.* E **59** 2594
[11] Sengupta S, Nielaba P and Binder K 2000 *Europhys. Lett.* **50** 668
[12] Alder B J and Wainwright T E 1962 *Phys. Rev.* **127** 359
[13] Hoover W G and Ree F H 1968 *J. Chem. Phys.* **49** 3609
[14] Mermin N D 1968 *Phys. Rev.* **176** 250
[15] Sengupta S, Nielaba P and Binder K 2000 *Phys. Rev.* E **61** 6294
[16] Santos A, López de Haro M and Bravo Yuste S 1995 *J. Chem. Phys.* **103** 4622
[17] Alder B J, Hoover W G and Young D A 1968 *J. Chem. Phys.* **49** 3688
[18] Zollweg J A and Chester G V 1992 *Phys. Rev.* B **46** 11 187
[19] Landau D P and Binder K 2000 *A Guide to Monte Carlo Simulations in Statistical Physics* (Cambridge: Cambridge University Press)
[20] Binder K 1981 *Z. Phys.* B **43** 119
[21] Kosterlitz J M 1974 *J. Phys. C: Solid State Phys.* **7** 1046
[22] Amit D J, Goldschmidt Y Y and Grinstein G 1980 *J. Phys. A: Math. Gen.* **13** 585
[23] Gupta R and Baillie C F 1992 *Phys. Rev.* B **45** 2883
[24] Janke W and Nather K 1993 *Phys. Rev.* B **48** 7419
[25] Olsson P 1994 *Phys. Rev. Lett.* **73** 3339
[26] Janke W 1997 *Phys. Rev.* B **55** 3580
[27] Fisher D S, Halperin B I and Morf R 1979 *Phys. Rev.* B **20** 4692
[28] Sengupta S, Nielaba P, Rao M and Binder K 2000 *Phys. Rev.* E **61** 1072